# Dynamic Nuclear Polarization Surface Enhanced NMR Spectroscopy

AARON J. ROSSINI,[†] ALEXANDRE ZAGDOUN,[†] MORENO LELLI,[†]
ANNE LESAGE,[†] CHRISTOPHE COPÉRET,[‡] AND
LYNDON EMSLEY[*,†]

[†]Centre de RMN a Tres Hauts Champs, Universite de Lyon (CNRS/ENS Lyon/UCB Lyon 1), 69100 Villeurbanne, France, and [‡]Department of Chemistry, Laboratory of Inorganic Chemistry, ETH Zurich, CH-8093, Zurich, Switzerland

## CONSPECTUS

Many of the functions and applications of advanced materials result from their interfacial structures and properties. However, the difficulty in characterizing the surface structure of these materials at an atomic level can often slow their further development. Solid-state NMR can probe surface structure and complement established surface science techniques, but its low sensitivity often limits its application. Many materials have low surface areas and/or low concentrations of active/surface sites. Dynamic nuclear polarization (DNP) is one intriguing method to enhance the sensitivity of solid-state NMR experiments by several orders of magnitude. In a DNP experiment, the large polarization of unpaired electrons is transferred to surrounding nuclei, which provides a maximum theoretical DNP enhancement of $\sim$658 for $^1$H NMR. In this Account, we discuss the application of DNP to enhance surface NMR signals, an approach known as DNP surface enhanced NMR spectroscopy (DNP SENS).



Enabling DNP for these systems requires bringing an exogeneous radical solution into contact with surfaces without diluting the sample. We proposed the incipient wetness impregnation technique (IWI), a well-known method in materials science, to impregnate porous and particulate materials with just enough radical containing solution to fill the porous volume. IWI offers several advantages: it is extremely simple, provides a uniform wetting of the surface, and does not increase the sample volume or substantially reduce the concentration of the sample.

This Account describes the basic principles behind DNP SENS through results obtained for mesoporous and nanoparticulate samples impregnated with radical solutions. We also discuss the quantification of the overall sensitivity enhancements obtained with DNP SENS and compare that with ordinary room temperature NMR spectroscopy. We then review the development of radicals and solvents that give the best possible enhancements today. With the best polarizing mixtures, DNP SENS enhances sensitivity by a factor of up to 100, which decreases acquisition time by five orders of magnitude. Such enhancement enables the detailed and expedient atomic level characterization of the surfaces of complex materials at natural isotopic abundance and opens new avenues for NMR. To illustrate these improvements, we describe the successful application of DNP SENS to characterize hybrid materials, organometallic surface species, and metal−organic frameworks.
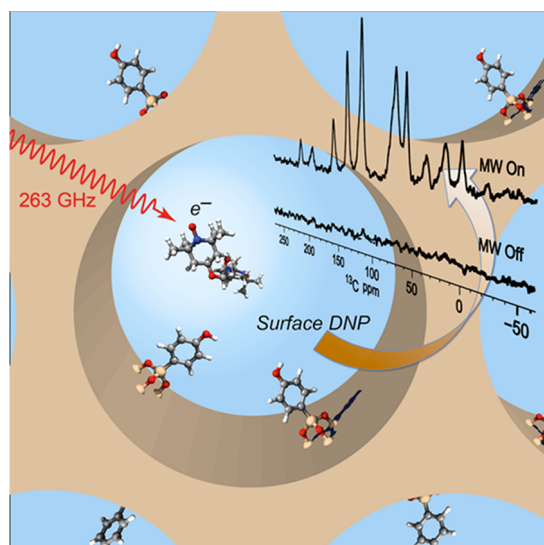
## Introduction

The ability to determine three-dimensional molecular structures from single crystals by diffraction methods has transformed molecular and materials science over the past 100 years, leading to the structure-based understanding of chemistry we have today. However, when the species of interest is at a surface, the problem of structure elucidation becomes much more challenging.

The rational development of new materials for applications as diverse as conversion/capture of atmospheric $CO_2$,

solar energy, gas storage/separation, hydrogen production, or advanced sensors requires structure−property relationships to be established.[1] Today, EXAFS, vibrational (IR and Raman), and electronic (UV−Vis) spectroscopies, together with surface science techniques (XPS, Auger, atomic force and electron microscopy) and mass spectrometry (SIMS) are used to characterize surfaces. However, methods for complete atomic level characterization have remained elusive unless high-vacuum techniques and well-defined crystalline phases are considered. Solid-state nuclear magnetic resonance (NMR) spectroscopy (in conjunction with other methods) could be the method of choice, but it is plagued by poor sensitivity.

NMR has intrinsically low sensitivity (compared to higher energy spectroscopies), which is further exacerbated for surface characterization by the small fraction of surface sites. For example, typical high surface area ($A = 800$ m$^2$/g) mesoporous silicas have a concentration of only $0.01−1.5$ mmol/g ($0.002−0.3$ mmol/mL) of surface functionalities, 1 or 2 orders of magnitude less than in a bulk molecular organic solid. The problem becomes worse as the surface area of the material or the density of surface sites is reduced (Figure 1).

Despite the challenge of low sensitivity, there is great interest in developing NMR for the characterization of surfaces. Following the development of modern cross-polarization magic angle spinning solid-state NMR experiments (CPMAS), it was soon realized that solid-state NMR could be a powerful probe of surface structure. In the early 1980s, Maciel and coworkers demonstrated that cross-polarization (CP) could be used to selectively observe NMR signals associated with the surface of silica.[2,3] Surface selective static CP experiments on metal oxides were also demonstrated by Ellis and Oldfied for quadrupolar $^{27}$Al and $^{17}$O nuclei, respectively.[4,5] CPMAS experiments were used for the acquisition of $^{13}$C and $^{31}$P spectra of molecules immobilized on polymer and silica surfaces.[3,6] With such spectra, it is often possible to determine the distribution of atomic environments, follow chemical transformations, probe dynamics, and propose structural models.

The characterization of single-site heterogeneous catalysts with solid-state NMR is a large focus of our research groups.[7−12] For highly receptive NMR nuclei (e.g., $^1$H, $^{19}$F, and $^{31}$P), the chemical structure, connectivity, and spatial proximity of surface species can be probed with multidimensional correlation experiments.[12,13] Pulse sequences which directly detect signals from dilute nuclei with nuclear spin $I = 1/2$ (e.g., $^{13}$C, $^{15}$N, $^{29}$Si) or quadrupolar nuclei ($I > 1/2$) are well established.[13,14] However, they are difficult to apply to surfaces since days of signal averaging are typically required for basic 1D spectra, unless the sample is isotopically
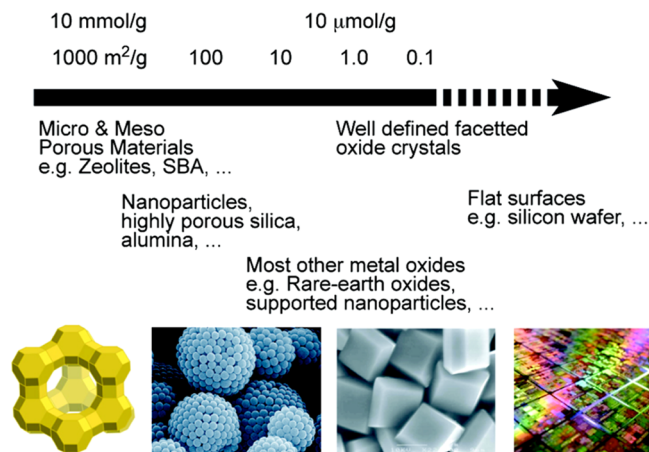


**FIGURE 1.** Some functional materials and their typical surface areas.

labeled, or fast MAS rates ($\nu_{rot} > 30$ kHz) and indirect detection are applied.[15] Indirect detection provides sensitivity enhancements of up to an order of magnitude; however, this is still insufficient to enable rapid characterization of many surface species.

The most promising techniques for improving the sensitivity of NMR experiments involve hyper-polarization of the nuclear spin states. Nuclei residing at surfaces have previously been hyper-polarized by reacting the surface with para-hydrogen[16] or by contacting optically polarized $^{129}$Xe gas with the surface.[17] Alternative signal detection schemes such as microcoils,[18] or magnetic resonance atomic force microscopy[19] have also been explored for thin films or surfaces.

One intriguing possibility for further increasing the sensitivity of solid-state NMR experiments on surface species is dynamic nuclear polarization (DNP).[20] In a DNP experiment, the large polarization of unpaired electrons is transferred to surrounding nuclei providing a maximum theoretical DNP enhancement ($\varepsilon$) of $\gamma_e/\gamma_x$, where $\gamma_e$ and $\gamma_x$ are the gyromagnetic ratios of the electron and the polarized nucleus, respectively ($\sim$658 for $^1$H). Enhancements are usually between 10 and 200; however, even modest signal enhancements can translate into spectacular reductions in experiment times, as the amount of time required for signal averaging is inversely proportional to the square of the enhancement. Here we discuss how DNP can be applied to enhance surface NMR signals in an approach referred to as DNP surface enhanced NMR spectroscopy (DNP SENS).

## A Brief History of DNP, and Basic Aspects of Modern High-Field DNP Experiments

The theory of DNP was developed by Overhauser in the 1950s and experimentally observed immediately after for
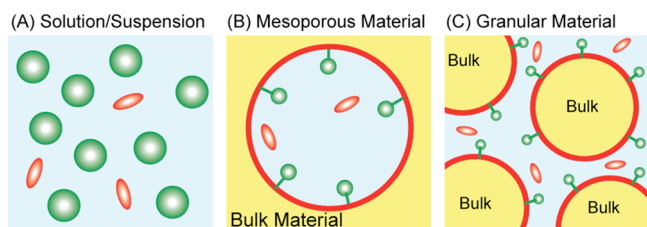
**FIGURE 2.** Schematics of methods for introducing stable radicals into systems for DNP solid-state NMR experiments. Green spheres represent target analytes, red lines indicate surface nuclei which may be polarized, red ellipsoids represent stable biradicals, the blue background represents a solvent or inert organic matrix, and yellow represents core nuclei of materials which are usually not polarized. (A) Bulk solution. (B) Impregnated porous material. (C) A granular/nonporous material impregnated with radical solution. Both (B) and (C) are used for DNP SENS.

lithium metal by Slichter.[21,22] This discovery lead to research into the spin physics of DNP in the 1960s which in turn lead to the application of DNP to materials such as coal, silicon, and diamond thin films, into the 1990s.[23-25] In these experiments, the source of polarization was usually intrinsic to the sample. The introduction of high field superconducting magnets around this time dramatically increased NMR sensitivity and resolution, and consequently, interest in DNP experiments waned because of their limitation to low magnetic fields (<3.5 T).

In the early 1990s, Griffin and co-workers introduced gyrotrons as high-power microwave sources suitable for DNP experiments at high magnetic fields (>5 T)[26] and combined them with cryogenic MAS probe technology for experiments below 100 K.[27] The combination of high power gyrotrons and low sample temperatures facilitates more complete saturation of the EPR transitions and can yield large DNP enhancements at high magnetic field. The idea of adding an external polarization source (a stable organic radical) was invoked early on,[28-30] but the full potential was only realized with the introduction of efficient biradical polarizing agents.[31] With such systems, $\varepsilon_H > 20$ can today routinely be obtained at 9.4 T.

The work of the Griffin group and the recent availability of commercial DNP solid-state NMR instruments[32] has recently lead to the application of DNP to many biomolecular systems. In such experiments, the biomolecule is usually dissolved or suspended in a radical containing water-glycerol solution (Figure 2A). This solution is then transferred to a rotor and cooled to ∼100 K. Glycerol serves as a cryo-protectant, preventing aggregation of the radical or crystallization upon freezing. Spectra of the sample are then acquired with continuous wave (CW) microwave irradiation that drives the DNP effect, enhancing the NMR signal.[20]
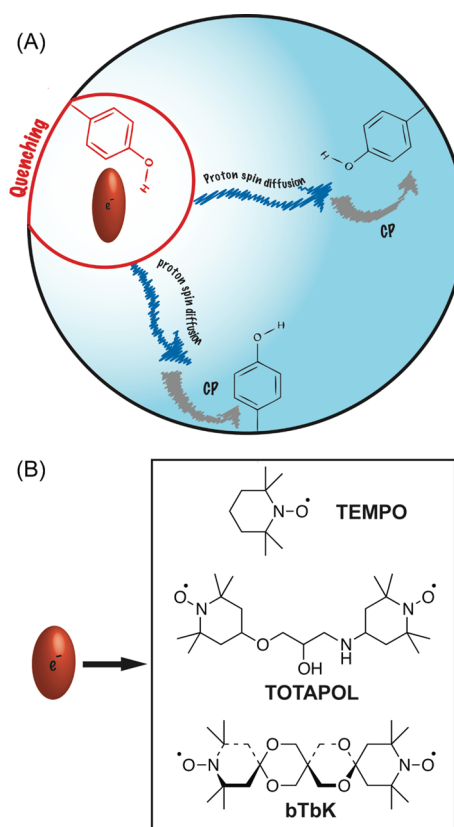


**FIGURE 3.** (A) Schematic (not to scale) model of DNP SENS for porous materials. A stable radical is introduced into the pores by impregnation. Enhanced polarization is transferred to the protons of the solvent and organic functionalities. CP is then used to transfer the enhanced polarization to dilute spins such as $^{13}$C. (B) Typical polarizing agents used for DNP.

## Dynamic Nuclear Polarization Surface Enhanced NMR Spectroscopy

Our interest in the characterization of catalyst materials led us to develop a DNP solid-state NMR method for the characterization of surfaces and materials.[33] Our aim was to develop a general method by focusing on intrinsically radical free materials. The key to enabling DNP for these systems is to bring an exogeneous radical solution into contact with surfaces without diluting the sample. We used the incipient wetness impregnation technique,[34] to impregnate porous and particulate materials with just enough radical containing solution to fill the porous volume (Figure 2B) or uniformly wet the surface of particulate materials (Figure 2C). For mesoporous silica materials, typically only 10 μL of radical solution is required to impregnate (and fill the porous volume) of around 12 mg of material. The elementary steps in DNP SENS are schematically illustrated in Figure 3. Proton spin diffusion uniformly distributes the enhanced proton polarization and CP is then used to

selectively polarize surface nuclei. However, nuclei too close to radicals will not be observed due to paramagnetic quenching (vide infra). This impregnation DNP technique has the advantage that it is extremely simple, and there is usually no dilution of the amount of solid material in the rotor (often the powdered sample is slightly compacted).

Initial DNP SENS experiments focused on phenol functionalized mesoporous silica having ca. 0.5 $\mu$mol phenol moieties/mg (**MatPhOH**, Figure 4B).[33] With conventional NMR, acquisition of 1D $^{13}$C CPMAS spectra at natural isotopic abundance typically requires a half day. DNP SENS yielded $\varepsilon_H$ ~25 (defined as the ratio of signal intensities of spectra acquired with and without microwave irradiation) and the proton DNP enhancement was then transferred to the surface carbon nuclei by CP. This enabled the acquisition of natural abundance $^{13}$C CPMAS spectra in only 0.5 h. This allowed for the observation of all the aromatic resonances of the phenol groups as well as byproducts and remaining templating surfactant. The signal enhancement from DNP SENS also enabled the rapid acquisition (4 h) of 2D dipolar $^1$H$-^{13}$C HETCOR spectra of **MatPhOH**.

$^{29}$Si DNP SENS CPMAS spectra of a variety of functionalized mesoporous and nanoparticulate silica materials were subsequently obtained (Figure 4D)[35] in only 0.5 h with high enough sensitivity to allow for observation of the surface functionalized silicon T sites (see below). $^1$H$-^{29}$Si dipolar HETCOR spectra were also acquired in minutes demonstrating the sensitivity enhancement provided by DNP SENS. Lafon et al. subsequently demonstrated that impregnation in conjunction with *direct* $^{29}$Si DNP enables observation of bulk silica sites.[36]

DNP SENS was also demonstrated for quadrupolar nuclei.[37] Figure 4E shows the $^{27}$Al DNP SENS CPMAS spectra of $\gamma$-alumina, with $\varepsilon_{Al\ CP}$ ~20. Since magnetization transfer by CP, necessary for surface selectivity, is usually very inefficient for quadrupolar nuclei,[14] low temperature DNP is especially beneficial here. DNP SENS enabled the rapid acquisition of a 2D CP multiple quantum magic angle spinning (MQMAS) spectrum. The same approach has recently been applied to the characterization of mesoporous alumina.[38]

## Quantifying Sensitivity Enhancements

$\varepsilon$ is of direct importance in evaluating the DNP process, but it is not necessarily relevant to assess the sensitivity enhancement provided with respect to a conventional NMR experiment.[39] It is this "overall sensitivity enhancement" ($\Sigma$) that is of real importance when evaluating the technique for the chemist. To quantify the gain in sensitivity provided
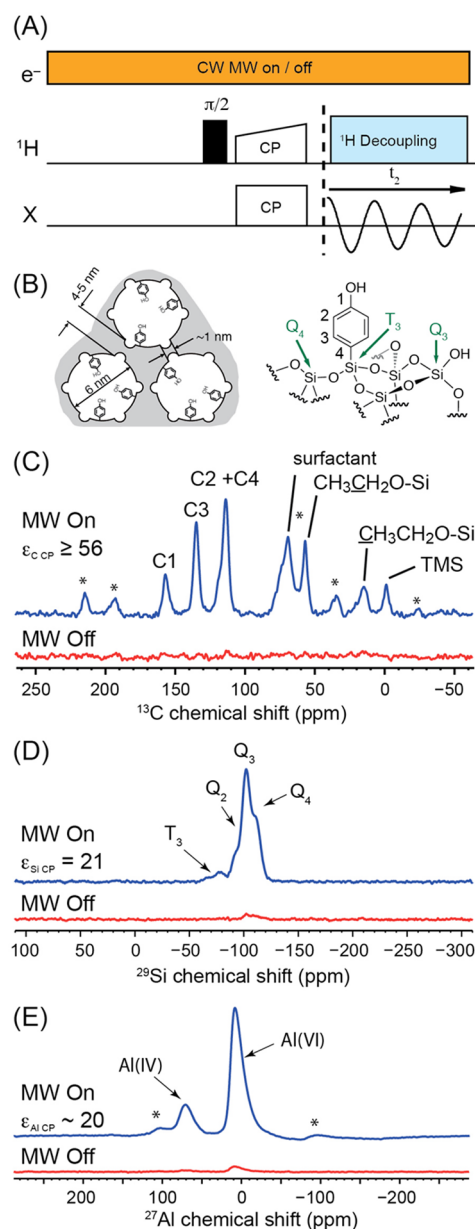


**FIGURE 4.** (A) CP pulse sequence used to acquire DNP SENS spectra with microwave irradiation to drive DNP. (B) Schematic structures of the hybrid mesoporous silica material (**MatPhOH**) and a chemical structure of the surface (right) with the assignment of the relevant carbon and silicon resonances. (C) $^{13}$C and (D) $^{29}$Si CPMAS spectra of **MatPhOH** impregnated with TOTAPOL in $D_2O/H_2O$ 90:10 solution acquired with (upper spectra) and without (lower spectra) microwave irradiation. (E) $^{27}$Al DNP SENS spectra of $\gamma$-alumina impregnated with TOTAPOL $D_2O/H_2O$ 90:10 solution. Adapted from refs 33, 35, and 37.

by 100 K DNP SENS experiments, as compared to room temperature experiments, the $^{29}$Si CPMAS signal per unit mass of **MatPhOH** impregnated with TOTAPOL solutions of varying concentration was measured (Figure 5).[40] The $^{29}$Si CP DNP enhancement ($\varepsilon_{Si\ CP}$) was found to peak at a value of 40 for a TOTAPOL concentration of 16 mM. However,
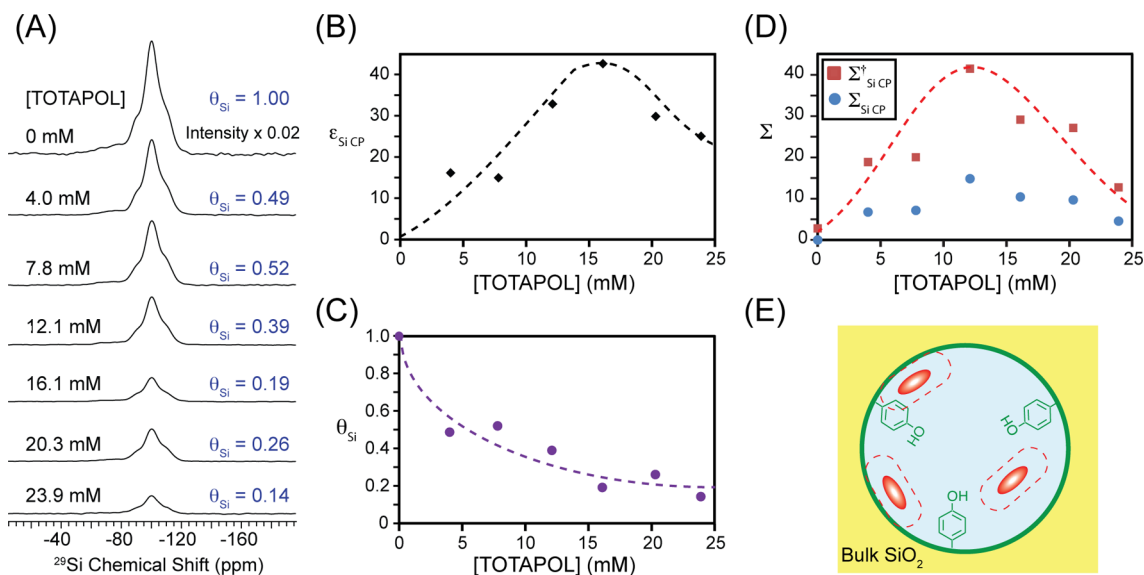
**FIGURE 5.** (A) $^{29}$Si CPMAS NMR spectra of **MatPhOH** impregnated with TOTAPOL solutions of varying concentration. The quenching factor ($\theta_{Si}$) is listed next to each spectrum. (B) $\varepsilon_{Si\,CP}$ and (C) $\theta_{Si}$ plotted as a function of TOTAPOL concentration. (D) The overall $^{29}$Si sensitivity enhancement with ($\Sigma^{\dagger}_{Si\,CP}$) and without ($\Sigma_{Si\,CP}$) Boltzmann enhancement. Dashed lines are added to guide the eye. (E) A schematic showing the distribution of radicals within **MatPhOH**. Radicals near to the surface induce quenching, reducing the magnitude of the $^{29}$Si (and $^{13}$C) NMR signal. Adapted from ref 40.

the largest absolute signal per unit mass was obtained for 12 mM TOTAPOL, for which $\varepsilon_{Si\,CP}$ was only 32. Larger signal per unit mass was obtained at lower radical concentration, indicating that the radicals are proximate to parts of the silica surface (Figure 5E). The signal loss is quantified by the quenching factor, $\theta_{Si}$, which is calculated by comparing the signal per unit mass from materials impregnated with pure water and TOTAPOL solutions.[40] For example, at 16 mM TOTAPOL, $\theta_{Si}$ was 0.20, indicating that ~80% of the surface $^{29}$Si NMR signal was rendered unobservable by the radical.

In order to assess the potential gain (or loss) in sensitivity from the DNP experiment, the combined effects of $\varepsilon_{Si\,CP}$, $\theta_{Si}$, and the acceleration of proton longitudinal relaxation rates by the radical should be taken into account. For experiments at ~105 K, there will also be additional thermal (Boltzmann) enhancement of the NMR signal by a factor 2.8 as compared to room temperature. The overall sensitivity enhancement can thus be expressed as:[40]

$$\Sigma^{\dagger}_{Si\,CP} = \left(\frac{298\,K}{105\,K}\right)(\theta_{Si})(\varepsilon_{Si\,CP})\sqrt{\frac{T_{1\,degassed}}{T_{1\,DNP}}}$$

A maximum $\Sigma^{\dagger}_{Si\,CP}$ of 42 was found for **MatPhOH** impregnated with 12 mM TOTAPOL. Other factors and methods for measuring DNP sensitivity enhancements have also been proposed.[41,42]

## Nonaqueous Solvents for DNP SENS

Initial DNP SENS experiments used aqueous TOTAPOL solutions as the polarizing medium. However, aqueous solutions prevent the application of DNP SENS to many materials (with hydrophobic surfaces or reactive centers for instance). Therefore, we investigated the possibility of using non-aqueous solvents for DNP.[43] The bTbK biradical[44] was first used as a polarization source for organic solvents, since it provides higher enhancements than TOTAPOL (*vide infra*) and is highly soluble in most organic solvents. A series of solvents were screened with the assumption that for the solution to provide efficient DNP it had to be fully frozen at 100 K, and have a low $^1$H concentration (<30 M). Solvents should also be inert toward both the radical and the analyte. Eight solvents were found to give good DNP enhancements, in particular 1,1,2,2-tetrachloroethane (TCE) and other halogenated solvents. The halogenated solvents also usually possess only a few distinct carbon sites in their NMR spectra, minimizing overlap with analyte resonances. In general, solvents with high proton concentrations and/or methyl groups gave lower enhancements.

## Improved Polarizing Agents

The DNP efficiency of the radical polarization source is a crucial factor in overall sensitivity, and it is important for low sensitivity applications on surfaces. Griffin and co-workers demonstrated that higher DNP enhancements can be
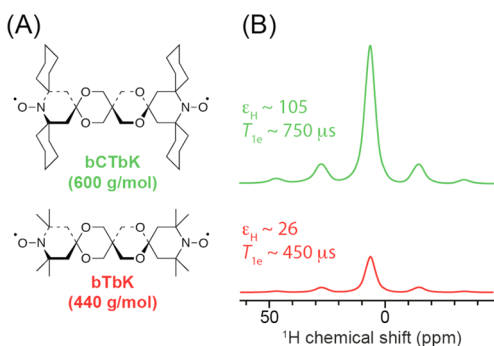
**FIGURE 6.** (A) Structures of bCTbK (upper) and bTbK (lower). $^1$H DNP MAS spectra of **MatPhOH** impregnated with TCE solutions of bCTbK (upper) and bTbK (lower). Adapted from ref 46.



**FIGURE 7.** $^{29}$Si DNP SENS of different phenol functionalized mesoporous materials: (A) hybrid material (10 240 scans, 2.8 h) for which the organic phenol moiety has been directly incorporated by a sol−gel process, and (B) mesoporous material obtained by postgrafting the phenolic units onto a SBA-15 matrix (26 624 scans, 7.4 h). The signals around 20 ppm correspond to surface SiMe$_3$ groups. (C) Structures of the T$_2$, T$_3$, Q$_3$ and Q$_4$ species present on the surfaces. Adapted from ref 35.

obtained by employing specially engineered biradicals, such as TOTAPOL, that take advantage of the cross effect (CE) mechanism.[31,45] In the model for the CE mechanism, a radical with Larmor frequency $\omega_{e1}$ is saturated, while a second electron at Larmor frequency $\omega_{e2}$ is not irradiated; the resulting difference in the polarization of the two electrons drives the DNP process, provided the frequency difference between $\omega_{e1}$ and $\omega_{e2}$ is equal to the nuclear Larmor frequency $\omega_0$: $|\omega_{e1} - \omega_{e2}| = \omega_0$. Proton spin diffusion can then distribute the polarization throughout the sample.[20] A further advance in biradical design was realized when Tordo, Griffin, and co-workers introduced bTbK, a rigid biradical with constrained orientations of the nitroxides (Figure 5).[44] bTbK was observed to provide larger $\varepsilon_H$ than TOTAPOL.

The biradical bCTbK was introduced with the notion of increasing DNP efficiency through longer electron relaxation times.[46] For nitroxides in glassy solvents at 100 K electron relaxation rates decrease as the molecular mass/volume of the radicals is increased.[47] bCTbK (Figure 6) has a molecular mass 1.4 times greater than bTbK, while retaining the favorable orientation of the two nitroxides. Both the effective transverse and longitudinal electron relaxation times for bCTbK in TCE at 100 K were found to be ~1.7 times longer than those for bTbK. The improved saturation of the EPR transitions afforded by the longer electronic relaxation times of bCTbK provides $\varepsilon_H$ values of ~100, which are 4 times larger than for bTbK (Figure 6). The high $\varepsilon_H$ for bCTbK enables the complete and expeditious characterization of surface species in functionalized materials.

## Probing the Surfaces of Porous Materials

Figure 7 shows $^{29}$Si DNP SENS spectra of a mesostructured organic−inorganic hybrid. A critical parameter, which determines the stability of such a material, is the topology of the linkages between the organic and inorganic parts.
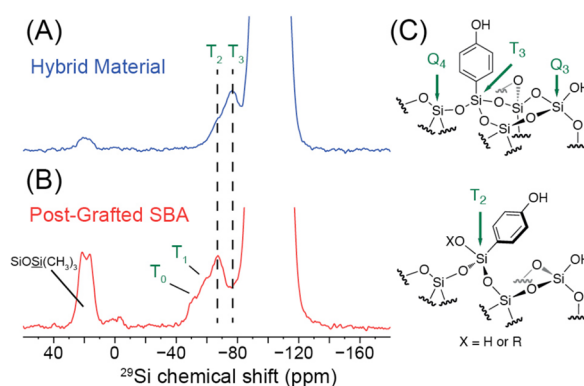
For silica-based materials $^{29}$Si chemical shifts depend on the number ($n$) of coordinating oxygen atoms bound to a second silicon atom and the number of organic fragments per Si atom (Q$_n$-sites bound to 4 oxygens, T$_n$-sites bound to 3 oxygens and 1 carbon, and D$_n$-sites bound to 2 oxygens and 2 carbons). Figure 7 shows this for materials containing phenol functionalities prepared through two routes: (i) the organic functionality is incorporated into the silica matrix during the synthesis of the material in the presence of a structure directing agent (direct synthesis)[48,49] or (ii) the organic moiety is grafted onto a previously prepared silica material, here SBA (postgrafting). Both materials have a SBA-like structure with large pores (~6 nm) and contain ~0.5 $\mu$mol/mg phenol. With $\varepsilon_{Si\ CP}$ of 21, only 3 h were needed to obtain spectra of sufficient quality for quantitative evaluation of the T site distribution (Figure 7).[35] For the direct synthesis, besides Q signals resulting from the silica matrix, the major signal corresponds to T$_3$, with a shoulder associated with minor amounts of T$_2$, showing the high level of condensation of the hybrid material. In contrast, with postgrafting synthesis, the major sites are T$_2$ and the minor sites are mainly associated with T$_1$ (monografted) and T$_0$ (adsorbed species).

The drastic sensitivity gains from DNP SENS enables monitoring of the surface postfunctionalization of a series of hybrid materials with multinuclear CPMAS spectra, as illustrated in Figure 8.[46] With bCTbK, $\varepsilon_H > 70$ was obtained, decreasing the experiment time by a factor ~5000. Notably, this enabled the rapid acquisition of natural abundance $^1$H−$^{15}$N CPMAS and 2D CP-HETCOR spectra (14 h each) for
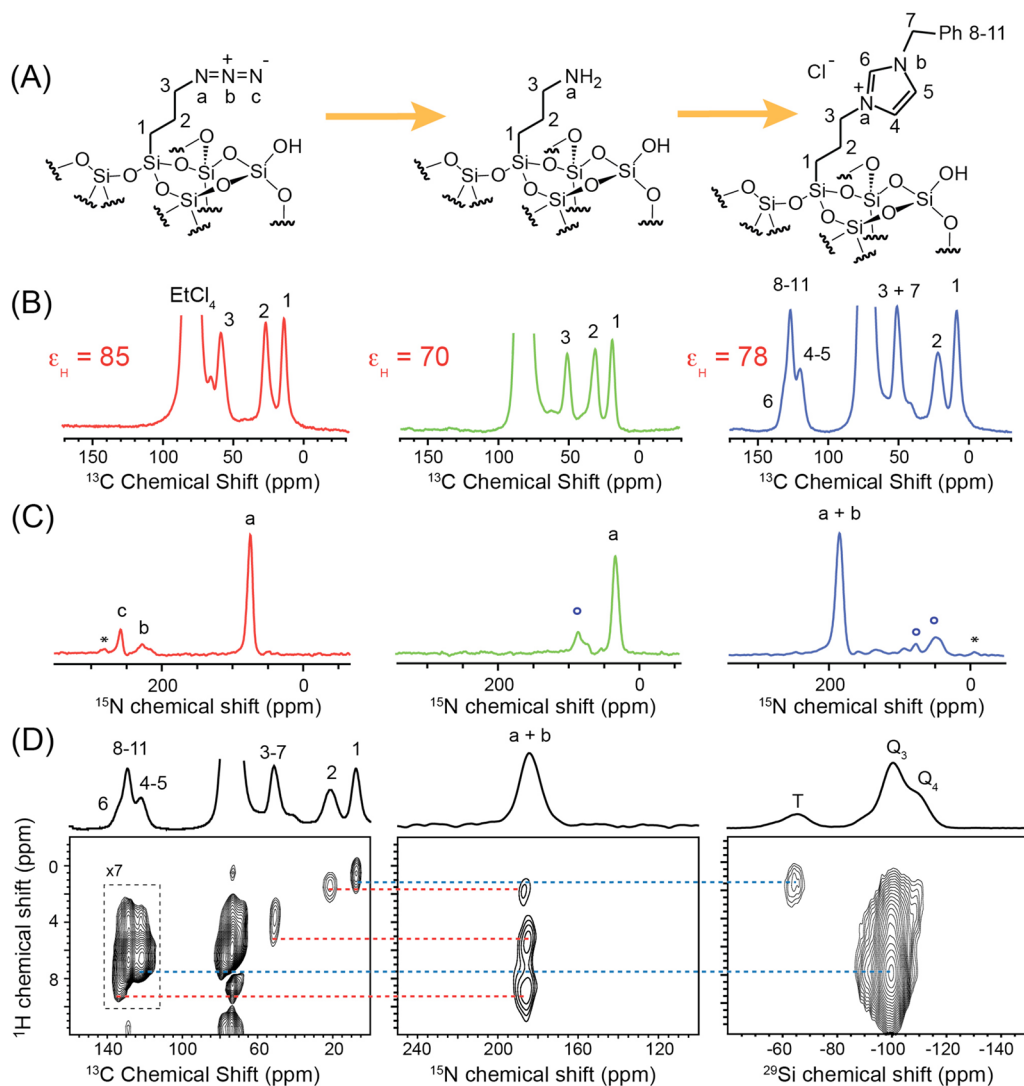
**FIGURE 8.** (A) Structure, (B) $^{13}C$ (C) $^{15}N$ DNP SENS CPMAS spectra of materials Mat-PrN$_3$, Mat-PrNH$_2$, and Mat-PrIm. (D) $^1H-^{13}C$, $^1H-^{15}N$, $^1H-^{29}Si$ DNP SENS two-dimensional HETCOR spectra of Mat-PrIm. The open circles indicate byproducts or incomplete conversion from the previous synthetic steps. 1D and 2D $^{15}N$ DNP SENS spectra were acquired with total experiment times of 14 h. Adapted from ref 46.

functionalities present at 1.2 $\mu$mol/mg (0.24 mmol/mL). Characteristic changes in the NMR spectra, reflecting the sequential chemical transformations, were observed for the series of systems. It was even possible to observe residual azido functionalities in the $^{15}N$ spectra, suggesting that a small (possibly inaccessible) fraction of surface sites is unreactive. The series of HETCOR spectra enabled the connectivity of the propyl-imidazolium moiety to be mapped.

In addition to the oxide based materials discussed above, DNP SENS was demonstrated to enhance NMR sensitivity for metal—organic framework (MOF) materials.[50] (In)-MIL-68 type MOFs (**1**−**3**) with functionalized organic linkers (Figure 9A) have pore diameters of ∼1.6 nm. Despite the much smaller pore sizes, which are similar in size to the bTbK biradical, impregnation could still deliver polarizing

mixture into the pores of **1** and **2**. However, $\varepsilon_{C\ CP}$ for the solvent and MOF resonances was observed to steadily increase as the impregnated materials were allowed for rest, likely due to slow diffusion of the bTbK radical into the material. For **1** and **2**, $\varepsilon_{C\ CP} > 12$ was obtained, which translated into $\Sigma \sim 3.5$. The relatively low $\Sigma$ was due to paramagnetic quenching of the NMR signal, however, high signal-to-noise ratio $^{13}C$ CPMAS could still be acquired in minutes, and the intensity of the $^{13}C$ resonances was reflective of the substitution pattern and stoichiometry of the linkers.

For **3**, a difference in the enhancement was observed for the solvent ($\varepsilon_{C\ CP} = 26$) and the MOF material ($\varepsilon_{C\ CP} = 4.8$). The proline groups of **3** block the radical from entering the material. Therefore, for **3**, the radical was restricted to the surface of the MOF particles (∼300 nm diameter from SEM
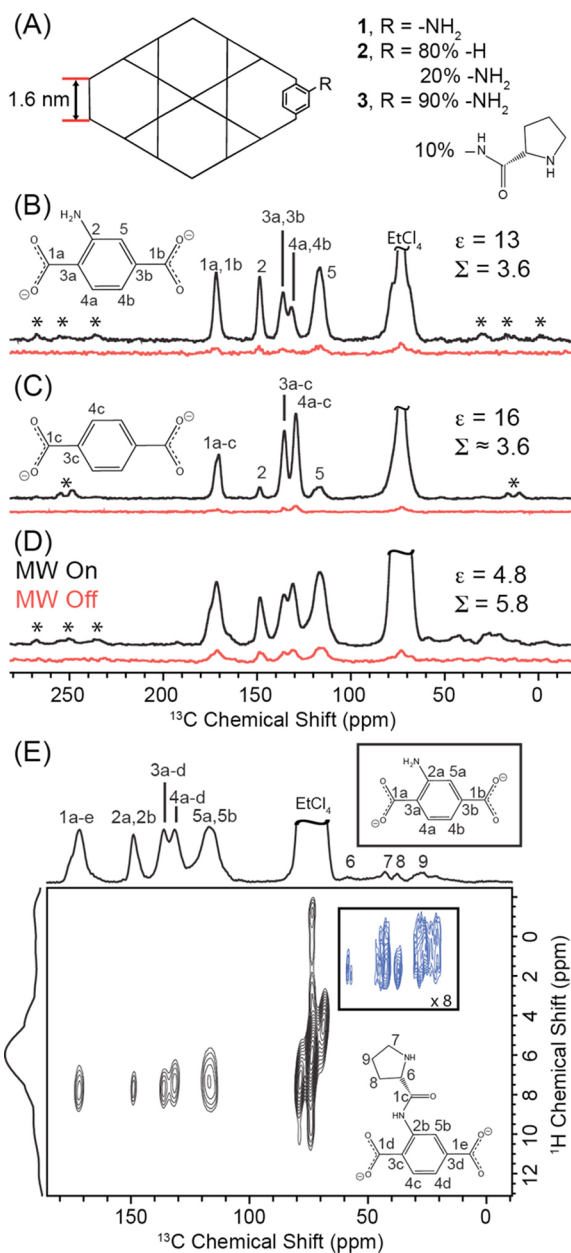
**FIGURE 9.** (A) Schematic structural model of the (In)-MIL-68 type MOFs **1**−**3**. (B−D) One-dimensional $^1H$−$^{13}C$ CPMAS spectra of MOFs **1**−**3**, respectively, recorded with (black) or without microwave irradiation (red) to induce DNP. The samples were impregnated with a 16 mm bTbK TCE solution. A total of 64 scans (A), or 128 scans (B and C) were accumulated. (D) Two-dimensional $^1H$−$^{13}C$ HETCOR spectrum of **3** acquired in 10.6 h. Adapted from ref 50.

images) and enhanced polarization entered into the MOF crystallites by spin diffusion from protons at the surface. This provides a modest DNP enhancement ($\varepsilon_{C\ CP} = 4.8$) but translates into a substantial sensitivity enhancement ($\Sigma = 5.8$) by eliminating paramagnetic quenching by excluding the radicals. This enabled the expedient acquisition (10.6 h) of a $^1H$−$^{13}C$ dipolar HETCOR spectrum with enough signal to observe the presence of the dilute proline groups, confirming their incorporation into the framework (Figure 9E). For **1**−**3** natural abundance $^{15}N$ CP/MAS spectra were also acquired in times from 20 min to 5 h.

## Conclusions and Future Directions

In summary, we have recently demonstrated how impregnation DNP can enhance the sensitivity of solid-state NMR for characterization of surfaces, leading to the DNP SENS technique. This approach can readily be applied to both porous and nonporous solids such as oxide-based materials. With the development of improved polarizing agents such as bCTbK, sensitivity enhancements >70 can now be routinely obtained, which translates into an acceleration of the acquisition time by 5000. This enables the complete and expedient characterization of high surface area materials with natural abundance $^{13}C$, $^{15}N$, and $^{29}Si$ solid-state NMR experiments. In the future, the combination of DNP SENS and isotopic labeling could enable experiments on very low surface area materials (<50 m$^2$/g). We have also recently demonstrated that impregnation DNP can be applied to micrometer size organic solids,[51] enabling DNP enhanced NMR of ordinary solids.

BIOGRAPHICAL INFORMATION

**Dr. Aaron Rossini** (Brantford, Canada, 1982). He obtained both B. Sc. (2005) and Ph.D. degrees in Chemistry (2010) from the University of Windsor (Canada) under the supervision of Prof. R. W. Schurko. His research interests as a postdoc focus on the development and applications of solid-state NMR for characterizing functional materials.

**Mr. Alexandre Zagdoun** (Paris, France, 1988). He obtained a Masters degree in Chemistry at the École Normale Supérieure de Lyon (2010) and is currently working on his Ph.D. on DNP SENS under the direction of Prof. Lyndon Emsley.

**Dr. Moreno Lelli** (Bologna, Italy, 1975). He obtained his undergraduate (1999) and Ph.D. degrees in chemistry from Scuola Normale Superiore of Pise (2002) under the supervision of Profs.

L. Di Bari and P. Salvadori. He was a postdoctoral fellow at the University of Florence with Prof. I. Bertini (2003–2009). Since 2009 he is a CNRS scientist developing NMR methods for the investigation of biomolecules and materials.

**Dr. Anne Lesage** (Ste. Colombe, France, 1969). She received her degree of "Ingénieur" in 1992 from the Ecole Centrale de Paris and completed her Ph.D. in the IBCP Lyon with Prof. M. VanderRest. In 1994, she became a CNRS scientist at the Ecole Normale Supérieure de Lyon, working with Lyndon Emsley on high-resolution solid-state NMR techniques.

**Prof. Christophe Copéret** (Belleville-sur-Saône, France, 1970). He was trained in chemistry and chemical engineering at CPE Lyon and then undertook his Ph.D. at Purdue University under the guidance of Prof. E. i. Negishi (1991–1996). After a postdoctoral stay at the Scripps Research Institute with Prof. K. B. Sharpless (1996–1997), he obtained a CNRS research position in 1998 in Lyon. Since November 2010, he holds a Professorship in Chemistry at the ETH Zürich, where he works at the frontiers of molecular, materials and surface chemistry, with the aim to design functional materials.

**Prof. Lyndon Emsley** (Durham, England, 1964). He studied undergraduate chemistry at Imperial College and then obtained a Ph.D. in Lausanne with Prof. G. Bodenhausen in 1991. He was then a Miller Fellow in Berkeley, working with Prof. A. Pines from 1991 to 1993. Since 1994, he is a Professor of Chemistry at the Ecole Normale Supérieure de Lyon, where he develops new methods for the study of materials and molecules by NMR spectroscopy.

### FOOTNOTES

### REFERENCES

1 Somorjai, G. A.; Frei, H.; Park, J. Y. Advancing the Frontiers in Nanocatalysis, Biointerfaces, and Renewable Energy Conversion by Innovations of Surface Techniques. *J. Am. Chem. Soc.* **2009**, *131*, 16589–16605.

2 Maciel, G. E.; Sindorf, D. W. SI-29 Nuclear Magnetic-Resonance Study of the Surface of Silica-Gel by Cross-Polarization and Magic-Angel Spinning. *J. Am. Chem. Soc.* **1980**, *102*, 7606–7607.

3 Maciel, G. E.; Sindorf, D. W.; Bartuska, V. J. Characterization of Silica-Attached Systems by Si-29 and C-13 Cross-Polarization and Magic-Angle Spinning Nuclear Magnetic-Resonance. *J. Chromatogr.* **1981**, *205*, 438–443.

4 Walter, T. H.; Turner, G. L.; Oldfield, E. O-17 Cross-Polarization NMR-Spectroscopy of Inorganic Solids. *J. Magn. Reson.* **1988**, *76*, 106–120.

5 Morris, H. D.; Ellis, P. D. Al-27 Cross-Polarization of Aluminas - The NMR-Spectroscopy of Surface Aluminum Atoms. *J. Am. Chem. Soc.* **1989**, *111*, 6045–6049.

6 Bemi, L.; Clark, H. C.; Davies, J. A.; Fyfe, C. A.; Wasylishen, R. E. Studies of Phosphorus(III) Ligands and Their Complexes of Ni(II), Pd(II), and Pt(II) Immobilized on Insoluble Supports By High-Resolution Solid-State P-31 NMR Using Magic-Angle Spinning Techniques. *J. Am. Chem. Soc.* **1982**, *104*, 438–445.

7 Chabanas, M.; Quadrelli, E. A.; Fenet, B.; Coperet, C.; Thivolle-Cazat, J.; Basset, J. M.; Lesage, A.; Emsley, L. Molecular insight into surface organometallic chemistry through the combined use of 2D HETCOR solid-state NMR spectroscopy and silsesquioxane analogues. *Angew. Chem., Int. Ed.* **2001**, *40*, 4493–4494.

8 Rataboul, F.; Baudouin, A.; Thieuleux, C.; Veyre, L.; Coperet, C.; Thivolle-Cazat, J.; Basset, J. M.; Lesage, A.; Emsley, L. Molecular understanding of the formation of surface zirconium Hydrides upon thermal treatment under hydrogen of [(SiO)Zr(CH(2)tBu)(3)] by using advanced solid-state NMR techniques. *J. Am. Chem. Soc.* **2004**, *126*, 12541–12550.

9 Blanc, F.; Coperet, C.; Thivolle-Cazat, J.; Basset, J. M.; Lesage, A.; Emsley, L.; Sinha, A. Schrock, R. R. Surface versus molecular siloxy ligands in well-defined olefin metathesis catalysts: [{(RO)(3)SiO}Mo(=NAr)(=CHtBu)(CH(2)tBu)]. *Angew. Chem., Int. Ed.* **2006**, *45*, 1216–1220.

10 Avenier, P.; Taoufik, M.; Lesage, A.; Solans-Monfort, X.; Baudouin, A.; de Mallmann, A.; Veyre, L.; Basset, J. M.; Eisenstein, O.; Emsley, L.; Quadrelli, E. A. Dinitrogen dissociation on an isolated surface tantalum atom. *Science* **2007**, *317*, 1056–1060.

11 Blanc, F.; Basset, J. M.; Coperet, C.; Sinha, A.; Tonzetich, Z. J.; Schrock, R. R.; Solans-Monfort, X.; Clot, E.; Eisenstein, O.; Lesage, A.; Emsley, L. Dynamics of silica-supported catalysts determined by combining solid-state NMR spectroscopy and DFT calculations. *J. Am. Chem. Soc.* **2008**, *130*, 5886–5900.

12 Blanc, F.; Coperet, C.; Lesage, A.; Emsley, L. High resolution solid state NMR spectroscopy in surface organometallic chemistry: access to molecular understanding of active sites of well-defined heterogeneous catalysts. *Chem. Soc. Rev.* **2008**, *37*, 518–526.

13 Lesage, A. Recent advances in solid-state NMR spectroscopy of spin I=1/2 nuclei. *Phys. Chem. Chem. Phys.* **2009**, *11*, 6876–6891.

14 Ashbrook, S. E. Recent advances in solid-state NMR spectroscopy of quadrupolar nuclei. *Phys. Chem. Chem. Phys.* **2009**, *11*, 6892–6905.

15 Wiench, J. W.; Bronnimann, C. E.; Lin, V. S. Y.; Pruski, M. Chemical shift correlation NMR spectroscopy with indirect detection in fast rotating solids: Studies of organically functionalized mesoporous silicas. *J. Am. Chem. Soc.* **2007**, *129*, 12076–12077.

16 Carson, P. J.; Bowers, C. R.; Weitekamp, D. P. The PASADENA effect at a solid surface: High-sensitivity nuclear magnetic resonance of hydrogen chemisorption. *J. Am. Chem. Soc.* **2001**, *123*, 11821–11822.

17 Long, H. W.; Gaede, H. C.; Shore, J.; Reven, L.; Bowers, C. R.; Kritzenberger, J.; Pietrass, T.; Pines, A.; Tang, P.; Reimer, J. A. High-Field Cross-Polarization NMR From Laser-Polarized Xenon to a Polymer Surface. *J. Am. Chem. Soc.* **1993**, *115*, 8491–8492.

18 Kentgens, A. P. M.; Bart, J.; van Bentum, P. J. M.; Brinkmann, A.; Van Eck, E. R. H.; Gardeniers, J. G. E.; Janssen, J. W. G.; Knijn, P.; Vasa, S.; Verkuijlen, M. H. W. High-resolution liquid- and solid-state nuclear magnetic resonance of nanoliter sample volumes using microcoil detectors. *J. Chem. Phys.* **2008**, *128*, 052202.

19 Poggio, M.; Degen, C. L. Force-detected nuclear magnetic resonance: recent advances and future challenges. *Nanotechnology* **2010**, *21*, 342001.

20 Maly, T.; Debelouchina, G. T.; Bajaj, V. S.; Hu, K. N.; Joo, C. G.; Mak-Jurkauskas, M. L.; Sirigiri, J. R.; van der Wel, P. C. A.; Herzfeld, J.; Temkin, R. J.; Griffin, R. G. Dynamic Nuclear Polarization at High Magnetic Fields. *J. Chem. Phys.* **2008**, *128*, 052211-1–19.

21 Overhauser, A. W. Polarization of Nuclei in Metals. *Phys. Rev.* **1953**, *92*, 411–415.

22 Carver, T. R.; Slichter, C. P. Polarization of Nuclear Spins in Metals. *Phys. Rev.* **1953**, *92*, 212–213.

23 Duijvestijn, M. J.; Vanderlugt, C.; Smidt, J.; Wind, R. A.; Zilm, K. W.; Staplin, D. C. C-13 NMR-Spectroscopy in Diamonds Using Dynamic Nuclear Polarization. *Chem. Phys. Lett.* **1983**, *102*, 25–28.

24 Wind, R. A.; Duijvestijn, M. J.; Vanderlugt, C.; Manenschijn, A.; Vriend, J. Applications of Dynamic Nuclear-Polarization in C-13 NMR in Solids. *Prog. Nucl. Magn. Reson. Spectrosc.* **1985**, *17*, 33–67.

25 Lock, H.; Maciel, G. E.; Johnson, C. E. Natural Abundance C-13 Dynamic Nuclear-Polarization Experiments on Chemical Vapor-Deposited Diamond Film. *J. Mater. Res.* **1992**, *7*, 2791–2797.

26 Becerra, L. R.; Gerfen, G. J.; Temkin, R. J.; Singel, D. J.; Griffin, R. G. Dynamic Nuclear-Polarization with a Cyclotron-Resonance Maser at 5-T. *Phys. Rev. Lett.* **1993**, *71*, 3561–3564.

27 Hall, D. A.; Maus, D. C.; Gerfen, G. J.; Inati, S. J.; Becerra, L. R.; Dahlquist, F. W.; Griffin, R. G. Polarization-enhanced NMR spectroscopy of biomolecules in frozen solution. *Science* **1997**, *276*, 930–932.

28 Hwang, C. F.; Hill, D. A. New Effect In Dynamic Polarization. *Phys. Rev. Lett.* **1967**, *18*, 110–112.

29 Afeworki, M.; McKay, R. A.; Schaefer, J. Selective Observation of the Interface of Heterogeneous Polycarbonate Polystyrene Blends by Dynamic Nuclear-Polarization C-13 NMR-Spectroscopy. *Macromolecules* **1992**, *25*, 4084–4091.

30 Hu, J. Z.; Solum, M. S.; Wind, R. A.; Nilsson, B. L.; Peterson, M. A.; Pugmire, R. J.; Grant, D. M. 1H and 15N Dynamic Nuclear Polarization Studies of Carbazole. *J. Phys. Chem. A* **2000**, *104*, 4413–4420.

31 Song, C. S.; Hu, K. N.; Joo, C. G.; Swager, T. M.; Griffin, R. G. TOTAPOL: A biradical polarizing agent for dynamic nuclear polarization experiments in aqueous media. *J. Am. Chem. Soc.* **2006**, *128*, 11385–11390.

32 Rosay, M.; Tometich, L.; Pawsey, S.; Bader, R.; Schauwecker, R.; Blank, M.; Borchard, P. M.; Cauffman, S. R.; Felch, K. L.; Weber, R. T.; Temkin, R. J.; Griffin, R. G.; Maas, W. E. Solid-state dynamic nuclear polarization at 263 GHz: spectrometer design and experimental results. *Phys. Chem. Chem. Phys.* **2010**, *12*, 5850–5860.

33 Lesage, A.; Lelli, M.; Gajan, D.; Caporini, M. A.; Vitzthum, V.; Mieville, P.; Alauzun, J.; Roussey, A.; Thieuleux, C.; Mehdi, A.; Bodenhausen, G.; Copéret, C.; Emsley, L. Surface Enhanced NMR Spectroscopy by Dynamic Nuclear Polarization. *J. Am. Chem. Soc.* **2010**, *132*, 15459–15461.

34 *Synthesis of Solid Catalysts*, 1st ed.; de Jong, K. P., Ed.; Wiley-VCH: Weinheim, 2009.

35 Lelli, M.; Gajan, D.; Lesage, A.; Caporini, M. A.; Vitzthum, V.; Mieville, P.; Heroguel, F.; Rascon, F.; Roussey, A.; Thieuleux, C.; Boualleg, M.; Veyre, L.; Bodenhausen, G.; Copéret,

C.; Emsley, L. Fast Characterization of Functionalized Silica Materials by Silicon-29 Surface-Enhanced NMR Spectroscopy Using Dynamic Nuclear Polarization. *J. Am. Chem. Soc.* **2011**, *133*, 2104–2107.

36 Lafon, O.; Rosay, M.; Aussenac, F.; Lu, X.; Tre_bosc, J.; Cristini, O.; Kinowski, C.; Touati, N.; Vezin, H.; Amoureux, J. P. Beyond the Silica Surface by Direct Silicon-29 Dynamic Nuclear Polarization. *Angew. Chem., Int. Ed.* **2011**, *50*, 8367–8370.

37 Vitzthum, V.; Mieville, P.; Carnevale, D.; Caporini, M. A.; Gajan, D.; Coperet, C.; Lelli, M.; Zagdoun, A.; Rossini, A. J.; Lesage, A.; Emsley, L.; Bodenhausen, G. Dynamic nuclear polarization of quadrupolar nuclei using cross polarization from protons: surface-enhanced aluminium-27 NMR. *Chem. Commun.* **2012**, *48*, 1988–1990.

38 Lee, D.; Takahashi, H.; Thankamony, A. S. L.; Dacquin, J. P.; Bardet, M.; Lafon, O.; De Paëpe, G. Enhanced Solid-State NMR Correlation Spectroscopy of Quadrupolar Nuclei Using Dynamic Nuclear Polarization. *J. Am. Chem. Soc.* **2012**, *134*, 18491–18494.

39 Thurber, K. R.; Wai-Ming, Y.; Tycko, R. Low-temperature dynamic nuclear polarizatoin at 9.4 T with a 30 mW microwave source. *J. Magn. Reson.* **2010**, *204*, 303–313.

40 Rossini, A. J.; Zagdoun, A.; Lelli, M.; Gajan, D.; Rascon, F.; Rosay, M.; Maas, W. E.; Coperet, C.; Lesage, A.; Emsley, L. One hundred fold overall sensitivity enhancements for Silicon-29 NMR spectroscopy of surfaces by dynamic nuclear polarization with CPMG acquisition. *Chem. Sci.* **2012**, *3*, 108–115.

41 Vitzthum, V.; Borcard, F.; Jannin, S.; Morin, M.; Mieville, P.; Caporini, M. A.; Sienkiewicz, A.; Gerber-Lemaire, S.; Bodenhausen, G. Fractional Spin-Labeling of Polymers for Enhancing NMR Sensitivity by Solvent-Free Dynamic Nuclear Polarization. *ChemPhysChem* **2011**, *12*, 2929–2932.

42 Takahashi, H.; Lee, D.; Dubois, L.; Bardet, M.; Hediger, S.; De Paëpe, G. Rapid Natural-Abundance 2D 13C—13C Correlation Spectroscopy Using Dynamic Nuclear Polarization Enhanced Solid-State NMR and MatrixFree Sample Preparation. *Angew. Chem., Int. Ed.* **2012**, *124*, 11936–11939.

43 Zagdoun, A.; Rossini, A. J.; Gajan, D.; Bourdolle, A.; Ouari, O.; Rosay, M.; Maas, W. E.; Tordo, P.; Lelli, M.; Emsley, L.; Lesage, A.; Copéret, C. Nonaqueous Solvents for DNP Spectroscopy. *Chem. Commun.* **2011**, *48*, 654–656.

44 Matsuki, Y.; Maly, T.; Ouari, O.; Karoui, H.; Le Moigne, F.; Rizzato, E.; Lyubenova, S.; Herzfeld, J.; Prisner, T.; Tordo, P.; Griffin, R. G. Dynamic Nuclear Polarization with a Rigid Biradical. *Angew. Chem., Int. Ed.* **2009**, *48*, 4996–5000.

45 Hu, K. N.; Yu, H. H.; Swager, T. M.; Griffin, R. G. Dynamic Nuclear Polarization with Biradicals. *J. Am. Chem. Soc.* **2004**, *126*, 10844–10845.

46 Zagdoun, A.; Casano, G.; Ouari, O.; Lapadula, G.; Rossini, A. J.; Lelli, M.; Baffert, M.; Gajan, D.; Veyre, L.; Maas, W. E.; Rosay, M.; Weber, R. T.; Thieuleux, C.; Coperet, C.; Lesage, A.; Tordo, P.; Emsley, L. A Slowly Relaxing Rigid Biradical for Efficient Dynamic Nuclear Polarization Surface-Enhanced NMR Spectroscopy: Expeditious Characterization of Functional Group Manipulation in Hybrid Materials. *J. Am. Chem. Soc.* **2012**, *134*, 2284–2291.

47 Sato, H.; Kathirvelu, V.; Fielding, A.; Blinco, J. P.; Micallef, A. S.; Bottle, S. E.; Eaton, S. S.; Eaton, G. R. Impact of molecular size on electron spin relaxation rates of nitroxyl radicals in glassy solvents between 100 and 300K. *Mol. Phys.* **2007**, *105*, 2137–2151.

48 Corriu, R. J. P.; Mehdi, A.; Reye, C. Molecular chemistry and nanosciences: on the way to interactive materials. *J. Mater. Chem.* **2005**, *15*, 4285–4294.

49 Hoffmann, F.; Cornelius, M.; Morell, J.; Froba, M. Silica-based mesoporous organic-inorganic hybrid materials. *Angew. Chem., Int. Ed.* **2006**, *45*, 3216–3251.

50 Rossini, A. J.; Zagdoun, A.; Lelli, M.; Canivet, J.; Aguado, S.; Ouari, O.; Tordo, P.; Rosay, M.; Maas, W. E.; Coperet, C.; Farrusseng, D.; Emsley, L.; Lesage, A. Dynamic Nuclear Polarization Enhanced Solid-State NMR Spectroscopy of Functionalized Metal-Organic Frameworks. *Angew. Chem., Int. Ed.* **2012**, *51*, 123–127.

51 Rossini, A. J.; Zagdoun, A.; Hegner, F. S.; Schwarzwälder, M.; Gajan, D.; Copéret, C.; Lesage, A.; Emsley, L. Dynamic Nuclear Polarization NMR Spectroscopy of Microcrystalline Solids. *J. Am. Chem. Soc.* **2012**, *134*, 16899–16908.